

# Erosion Measurements by Cavity Ring-Down Spectroscopy for the VHITAL Program

IEPC-2005-299

*Presented at the 29<sup>th</sup> International Electric Propulsion Conference, Princeton University,  
October 31 – November 4, 2005*

Azer P. Yalin<sup>\*</sup>, Vijaya Surla<sup>†</sup>, and John D. Williams<sup>‡</sup>  
*Colorado State University, Fort Collins, Colorado, 80523*

**Abstract:** We report the use of cavity ring-down spectroscopy (CRDS) as a diagnostic tool to study sputter erosion of the VHITAL (Very High  $I_{sp}$  Thruster with Anode Layer) thruster. The lifetime of the VHITAL thruster is largely governed by sputter erosion of guard-rings and other critical components. The CRDS technique will be used to measure sputtered molybdenum in the plume of the thruster for various thruster operating conditions. Because the sputter rates of interest are relatively low (material erosion rates are  $\sim 0.1\text{-}10\ \mu\text{m}/\text{hour}$ ), a sensitive measurement technique such as CRDS is required. Our group has recently demonstrated the use of CRDS for sputter erosion studies. Here, we describe our bench-top sputtering setup consisting of an ion beam and target which we use for diagnostic development. We present CRDS measurements of sputtered molybdenum number density and velocity, including the dependence on number density on beam current, and comparison with a numerical sputter model. We present cavity hardware designs and bench-top testing for CRDS implementation on the VHITAL thruster. Challenges for the thruster implementation include maintaining cavity alignment and stability for the relatively long ( $\approx 3\text{m}$ ) optical-axis, and minimizing the reduction of effective cavity finesse (and CRDS sensitivity) due to mirror contamination from condensed bismuth or sputtered products.

## Nomenclature

$A_{ki}$	=	Einstein $A$ coefficient, 1/s
$Abs_{Eff}$	=	Effective absorbance
$c$	=	Speed of light, $2.998 \times 10^8$ m/s
$g_i$	=	Degeneracy of state $i$
$I_{sp}$	=	Specific impulse, s
$k(\nu)$	=	Absorption coefficient, $\text{m}^{-1}$
$k_{eff}(\nu)$	=	Effective absorption coefficient, $\text{m}^{-1}$
$L(\nu)$	=	Laser lineshape, $\text{Hz}^{-1}$
$l$	=	Length of the ring-down cavity, m
$N_i$	=	Lower state concentration, $\text{m}^{-3}$
$R$	=	Mirror reflectivity
ROC	=	Mirror radius-of-curvature, m
$S(t, \nu)$	=	Ring-down signal
$\nu$	=	Laser frequency, Hz
$\nu_{ki}$	=	Transition frequency, 1/s
$\tau$	=	Ring-down time, s
$\tau_0$	=	Empty cavity ring-down time, s

---

<sup>\*</sup> Assistant Professor, Mechanical Engineering, [ayalin@engr.colostate.edu](mailto:ayalin@engr.colostate.edu).

<sup>†</sup> Graduate Student, Mechanical Engineering, [vijay.surla@colostate.edu](mailto:vijay.surla@colostate.edu).

<sup>‡</sup> Assistant Professor, Mechanical Engineering, [johnw@engr.colostate.edu](mailto:johnw@engr.colostate.edu).

## I. Introduction

A primary objective of the overall VHITAL (Very High  $I_{sp}$  Thruster with Anode Layer) program<sup>1,2</sup> is to determine the expected thruster lifetime, which is largely governed by sputter erosion of guard-rings and other critical components. The lifetime determination approach is based on deploying several complementary diagnostic techniques in concert with numerical modeling. The experimental diagnostics will include applications of cavity ring-down spectroscopy (CRDS) and surface layer activation (SLA)<sup>3</sup>. The most critical sputter erosion is expected to occur at the guard-rings, for which several materials, including molybdenum and graphite, are being considered.

Although sputter erosion is the primary life-limiting process, the actual rates of sputter erosion (and number densities of sputtered particles) are relatively low, so that sensitive diagnostic techniques such as CRDS must be employed. In the VHITAL program, the CRDS diagnostic will be used to directly measure the (path-integrated) number densities of molybdenum sputter products in the plume of the thruster. The CRDS measurements will provide information on the dependence of the sputter erosion on thruster operating conditions. The measurement results will also be used to validate numerical erosion (lifetime) models, which can then be extended to simulate other sputtering materials of interest (as long as basic sputter yield data is available).

In this paper we present bench-top demonstrations and validation of the CRDS measurement approach. The bench-top configuration has been used to perform demonstrative measurements of sputtered molybdenum number density and velocity, including the dependence on beam current, and validation with a numerical sputter model. We also present designs and address issues connected to future implementations on the VHITAL thruster. Challenges associated with CRDS implementation for studies of the VHITAL thruster include: maintaining cavity alignment and stability for the relatively long ( $\approx 3\text{m}$ ) axis of the Jet Propulsion Laboratory (JPL) chamber, and minimizing the reduction of effective cavity finesse (and CRDS sensitivity) due to mirror contamination from condensed bismuth or sputter products.

## II. Cavity Ring-Down Spectroscopy (CRDS)

CRDS is a highly sensitive laser-based absorption technique<sup>4,5</sup> that is directly quantifiable and thus well suited to measurements of low concentrations of sputtered particles. It is an absorption technique, so that unlike fluorescence and emission measurements, ground states are measurable and there are no quenching interferences. Measuring ground states is advantageous since the ground states typically contain a large fraction of the overall species population. In this way, the signals tend to be larger and, in comparison to signals from excited states, can be more accurately related to the desired overall species population. As shown in Fig. 1, the basic idea is to house the absorbing sample (i.e. the sputtered atoms) within a high-finesse optical cavity formed from high-reflectivity mirrors ( $R \sim 0.9999$ ). The interrogating laser beam is coupled into the optical cavity where it “bounces” many times back-and-forth between the mirrors. Owing to the high reflectivity, the light within the cavity makes many passes (e.g.  $\sim 10^4$  passes for  $R \sim 0.9999$ ) within the cavity, and the effective path length and sensitivity is greatly increased. A detector placed behind the cavity measures the temporal decay of optical intensity within the cavity. The difference in the temporal decay rate with and without the absorber (or with the laser tuned on/off the resonance) yields the sample concentration. The technique has been used widely for the measurements of trace species in flames, plasmas, and the atmosphere, and we have recently pioneered its use for sputter measurements for electric propulsion applications<sup>6-8</sup>.

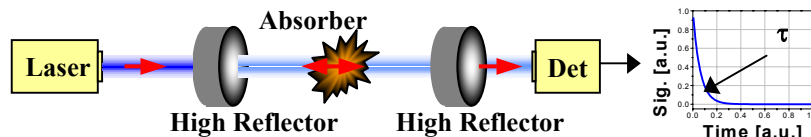


**Figure 1. Schematic diagram of cavity ring-down spectroscopy (CRDS). Laser light is coupled into a high reflectivity cavity where it bounces back and forth many times. A detector behind the cavity measures the decay of the light intensity inside the cavity which may be related to the concentration of the absorbing species.**

The technique affords high sensitivity owing to a combination of long effective path length and insensitivity to laser energy fluctuations. Under appropriate conditions, the ring-down signal  $S(t, \nu)$  decays single-exponentially<sup>9,10</sup> versus time as:

$$S(t, \nu) = S_0 \exp[-t/\tau(\nu)] \quad (1)$$

$$1/\tau(\nu) = \frac{c}{l} \left[ \int k_{\text{eff}}(x, \nu) dx + (1-R) \right] ; \quad k_{\text{eff}}(\nu) \equiv \int_{-\infty}^{+\infty} L(\nu' - \nu) k(\nu') d\nu'$$

where  $\tau$  is the 1/e time of the decay (termed the ring-down time),  $c$  is the speed of light,  $l$  is the cavity length,  $k_{\text{eff}}(\nu)$  is the effective absorption coefficient,  $\nu$  is the laser frequency,  $1-R$  is the effective mirror loss (including scattering and all cavity losses),  $L(\nu)$  is the laser lineshape function, and  $k(\nu)$  absorption coefficient. (If the absorber is uniformly present over a column length  $l_{\text{abs}}$ , then  $\int k_{\text{eff}}(x, \nu) dx$  can be replaced with the product  $k_{\text{eff}}(\nu)l_{\text{abs}}$ .) As in conventional absorption, the effective absorption coefficient accounts for line broadening arising from the laser lineshape. In practice, the measured ring-down signal is fitted with an exponential, and the ring-down time  $\tau$  is extracted. Combining  $\tau$  with the “empty cavity ring-down time”,  $\tau_0$  (which in practice is measured by detuning the laser) allows determination of the (effective) sample absorbance,  $Abs_{\text{eff}}$ , and (effective) absorption coefficient,  $k_{\text{eff}}$ :

$$Abs_{\text{eff}}(\nu) \equiv l_{\text{abs}} k_{\text{eff}}(\nu) = \frac{l}{c} \left[ \frac{1}{\tau(\nu)} - \frac{1}{\tau_0} \right] \quad (2)$$

As in conventional absorption, both the laser and absorber lineshapes are needed to determine the actual absorbance (and number density) if the absorption is measured at a single wavelength. A more practical approach is to scan the laser frequency across the absorption line and to measure the frequency-integrated spectrum (i.e. the line area). Because the area of the effective absorbance spectrum is equivalent to the area of the (actual) absorbance spectrum, this method removes lineshape dependences. Assuming the absorption line parameters are known, the measured area  $\int Abs_{\text{eff}}(\nu) d\nu$  of a transition from lower state  $i$  to upper state  $k$  can be readily converted to the path-integrated concentration of the lower state  $\int N_i dx$  as:

$$\int N_i dx = 8\pi \frac{g_i}{g_k} \frac{\nu_{ki}^2}{A_{ki} c^2} \left( \int Abs_{\text{eff}}(\nu) d\nu \right) \quad (3)$$

where  $g_i, g_k$  are the level degeneracies,  $\nu_{ki}$  is the transition frequency,  $A_{ki}$  is the transition Einstein  $A$  coefficient, and  $c$  is the speed of light. Actual concentration can be determined from the path-integrated concentration in several ways: assume a uniform concentration profile over a known column length,  $l_{\text{abs}}$ , as is done in this work; perform scans at different chords and use an Abel inversion for axisymmetric cases; or use an assumed profile shape (with amplitude scaled by the experimental path-integrated value). We have recently demonstrated the use of CRDS to extract velocity information from the measured spectral lineshapes. The approach is based upon Doppler shifts due to velocity components along the optical axis<sup>8</sup>.

### III. Bench-Top Measurements

#### A. Experimental Setup

Fig. 2 shows a schematic diagram of the bench-top sputtering apparatus employed for CRDS diagnostic development at CSU<sup>6,7</sup>. The apparatus allows us to use CRDS to probe sputtered particles created by an ion beam incident upon a target. The key components are an ion beam and target, housed within a vacuum facility. A roughing and turbo-pump (Turbo-V550) are used to bring the pressure to approximately  $10^{-6}$  torr under no-flow conditions. A small argon flow (1 sccm) is used to feed the system. In the current experiments, the target is a molybdenum disc of diameter 8 cm. The molybdenum samples used in our experiments are obtained from 0.51 mm thick sheets that were arc-cast and cross-rolled and tested as received (without polishing). The ion beam is extracted from an 8-cm diameter structurally integrated thruster<sup>11</sup> obtained from NASA, and modified to operate on an inert gas, and to use refractory metal filaments for both the main and neutralizer cathodes in place of the hollow

cathodes used in the original design. In these experiments, the beam is normally incident upon the target. The thruster operates with an IonTech power supply (MPS 3000), with typical beam currents and voltages of about 100 mA, and 400-1000 V respectively. In our current measurements, we mask the ion beam so that it has an active area of 8 cm x 2.5 cm (with the 8 cm extent oriented parallel to the optical axis).

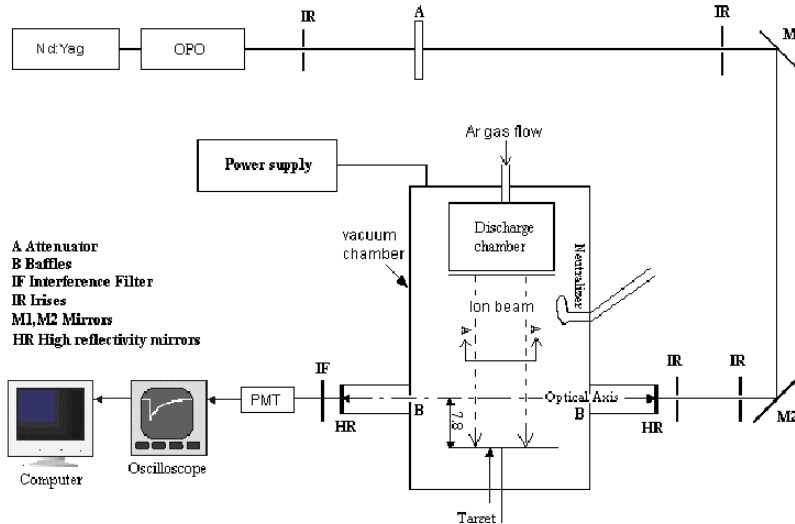


**Figure 2. Schematic diagram of sputtering apparatus and CRDS system. The ion beam is normally incident upon the target and optical axis is located 7.8 cm upstream of the target. The ring-down cavity has a length of 0.75 m, and uses 0.5-m radius of curvature mirrors. An OPO laser system is used as the light source, and a photomultiplier tube (PMT) detects the light exiting the cavity.**

The bench-top set-up uses a broadly tunable optical parametric oscillator (OPO) laser system (doubled idler) as the light source to probe optical transitions in the  $\sim 370\text{-}400$  nm region. In order to accommodate the full optical axis of the CRDS system, two extender arms (diameter 2", length 8.25") are used to house the mirrors. The mirrors are vacuum-sealed against adjacent O-rings. Adjustment of the mirror alignment is achieved using three set-screws that press against a brass ring on the back of the mirrors, allowing changes in the mirror angles by changing the compression of the O-ring. Laser parameters are: repetition rate = 10 Hz, pulse width  $\sim 7$  ns, pulse energy  $\sim 3$  mJ, and linewidth  $\sim 0.002$  nm. We use a linear ring-down cavity of length  $l=75$  cm with 50 cm radius-of-curvature (ROC) mirrors. Modeling results by Spuler et al.<sup>12</sup> indicate that this will be a near optimal cavity geometry in terms of spatial resolution (beam walk) and stability. The ring-down signal is collected behind the output mirror with a fast photomultiplier tube (Hamamatsu R3896). Ring-down signals are fit between 90%-10% of the peak amplitude. We use area (frequency-integrated) measurements of absorbance in our analyses. In order to prevent possible saturation (bleaching) effects, the laser energy is reduced with an attenuator to  $\sim 100$   $\mu\text{J}/\text{pulse}$  prior to cavity injection. For this input energy level, our spectra and number density measurements are unaffected by laser energy. (We have verified this by varying the laser input energy from 30-300  $\mu\text{J}/\text{pulse}$  and finding no change in the measured spectra.) We have confirmed that our CRDS measurements are not biased by the laser lineshape by using reduced temporal fitting windows<sup>10</sup>. We have also performed measurements with smaller targets (not shown in this work), and we find consistent results.

## B. CRDS Measurements of Sputtered Molybdenum

Spectroscopic models (including lineshape effects) are used to identify appropriate spectroscopic transitions and to quantitatively analyze data. A partial energy level diagram for molybdenum is shown in Fig. 3a. Our CRDS detection scheme for Mo is based upon probing strong optical absorption lines in the  $\sim 370\text{-}400$  nm region. The measured lines originate from the ground electronic state and have upper levels between 3 and 4 eV. We have measured absorption lines at 379.93 nm, 386.52 nm, and 390.41 nm. The areas of the measured absorption lines are fitted with Voigt peaks, the area of which yields the path-integrated number density of the ground state. After the ground state, the next lowest energy level is at 1.33 eV so that to a good approximation all population can be expected to reside in the ground state<sup>7</sup>. The inset of Fig. 3b shows a CRD spectrum for the 386.52 nm absorption line for a current of 18 mA. The main plot in Fig. 3b shows computed molybdenum concentrations as a function of

the beam current. The measured quantity in CRDS is the path-integrated concentration, and the concentrations displayed in Fig. 3b assume a uniform concentration over a path length of 8 cm (corresponding to the dimension of the ion beam). In order to obtain a detailed radial concentration profile, one could spatially scan the beam and use an Abel inversion.

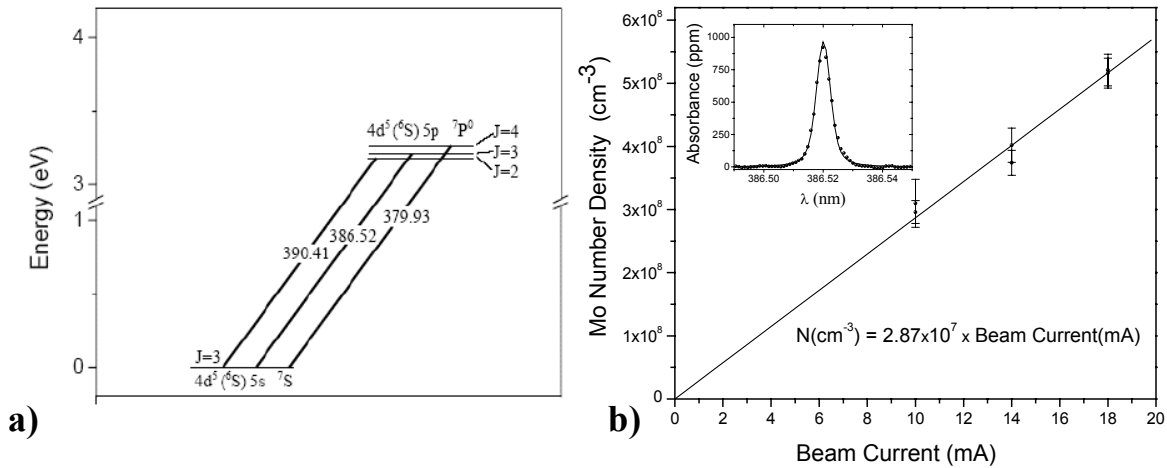


**Figure 3. a) Partial energy level diagram for molybdenum. Measured transitions are indicated (wavelengths are vacuum and in units of nm). All energy levels below 1 eV are included. Configurations, terms, J values, and wavelengths are from NIST. b) Dependence of molybdenum number density on beam current. A best-fit line (constrained to pass through the origin) is shown. Inset shows CRDS spectrum of the 386.52 nm line.**

### C. Validation and Detection Limits of Bench-Top System

We have performed several validations of our CRDS measurements. First, we have performed measurements of the variation of measured number density with beam current. Fig. 3b shows a plot of variation of molybdenum number density versus beam current. As the beam current is varied (at constant ion energy) the sputter yields are not altered; however, the current density increases. As expected, we observe a linear dependence (through the origin) of sputtered particle number density on beam current. We have also developed a simple sputter model to numerically predict path-integrated number densities as a function of experimental conditions. Using the model we compare measured path-integrated number densities with modeled values. The simplified sputtering model assumes a (diffuse) cosine-distribution for the differential sputter yield and uses the experimental beam current density ( $\sim 30\%$  uncertainty due to beam divergence and scattering effects) and target/optical-axis geometry. The model uses a finite element approach for both the target and optical axis, and computes the contribution of sputtered particles from each target element to each element along the optical axis. Summing the number densities along the extent of the optical axis gives the path-integrated number density. The results are insensitive to the grid size. For 750 eV ions we use a total sputter yield of  $0.9 \pm 0.3$  for molybdenum. The model also requires the angular profile of (the average inverse) ejected velocity of the sputtered particles, which we have found using the TRIM sputtering simulation software ( $\sim 20\%$  uncertainty). We have also used CRDS to measure the velocity profile<sup>8</sup> and find good agreement with the TRIM simulation results. Experimental spectra used for velocity measurements, obtained with two different geometries<sup>8</sup>, are shown in Figure 4.

While the simple numerical model agrees well with CRDS results for other species studied in our laboratory (e.g. iron, titanium, and aluminum), we find that for molybdenum the model predicts a number density about 1.5-3 times higher than measured by CRDS. (For beam conditions of 18 mA and 750 eV, the measured path-integrated number density is  $4.1 \pm 0.4 \times 10^9 \text{ cm}^{-2}$ , while the modeled value is  $13 \pm 6.4 \times 10^9 \text{ cm}^{-2}$ .) The discrepancy may in part be due to divergence and scattering of the ion beam (not included in the model); but is thought to be primarily due to the use of an incorrect sputter yield in the model. The molybdenum sputter yield depends on the details of the sample surface and preparation (and has not been directly measured for our sample). The variation in yields has been observed in other measurements performed at CSU using a quartz crystal microbalance (QCM) system. The overall good agreement between the CRDS and model provides validation of the measurement approach.

The sensitivity of the bench-top CRDS system is significantly better than what is thought to be required for measurements within the VHITAL thruster. The noise level in the current system is equivalent to an absorbance of  $\sim 2$  ppm, or a path-integrated concentration of Mo of  $\sim 6 \times 10^6 \text{ cm}^{-2}$ . Use of a dye-laser with a better spatial-mode is

expected to reduce the absorbance noise to  $\sim 0.1$  ppm which would correspond to a minimum detectable path-integrated concentration of Mo of  $\sim 3 \times 10^5 \text{ cm}^{-2}$ . The anticipated path-integrated concentration of Mo within the thruster is approximately  $10^8$ - $10^9 \text{ cm}^{-2}$ , so that even the current OPO based system should yield relatively high signal-to-noise concentration measurements.

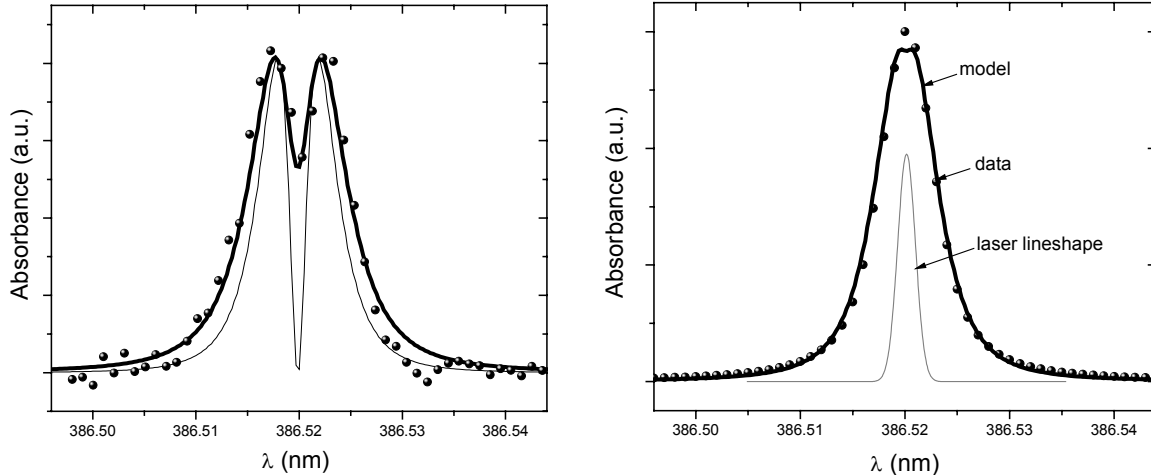


**Figure 4 Left:** Velocity measurement for Mo for geometry with a single direction of sputtered particles (at  $45^\circ$  to optical axis). Symbols - measured lineshape; Thick line – model fit with  $V_b=3500$  m/s; Thin line – model fit without laser convolution. **Right:** Velocity measurement for Mo with multi-directional sputtered particles. Symbols - measured lineshape; Thick line – model fit with  $V_b=3300$  m/s; Thin line – laser lineshape.

#### IV. VHITAL Implementation

The bench-top measurement scheme presented above forms the basis of the detection system under development for implementation on the VHITAL thruster at JPL in Phase 3 of the program. Implementation on the actual thruster in a vacuum chamber test facility will require the use of a longer cavity ( $\sim 3\text{m}$ ) as compared to that used in the CSU bench-top test facility ( $\sim 0.75\text{m}$ ). In this section, we describe the effect of the longer cavity on the ring-down stability, design of appropriate chamber arms and optical cavity for the JPL test facility, and planned measurements on the VHITAL thruster.

##### A. Cavity Length and Stability

Stability of an optical cavity can be characterized by the cavity g-parameter<sup>13</sup>, defined as  $g=1-l/ROC$ , where  $l$  is the length of the cavity and  $ROC$  is the radius-of-curvature of the cavity mirrors (assumed to be equal in this case). Fig. 5 shows numerical simulations of the dependences of beam size (at the center of the cavity) and beam walk as a function of cavity g-parameter<sup>12</sup>. From the point of view of our research, the beam size is generally not critical since we will be performing path-integrated measurements through the thruster plume, and the profile of sputter products within the plume is expected to be relatively wide (order 1-10s of cm). However, it is critical that we maintain cavity stability in order to have large and stable ring-down times necessary to enable high detection sensitivity. Our available mirrors have  $ROC=6$  m, yielding  $g=0.5$ , for the (JPL) cavity of length of 3m. Fig. 5 indicates that a g-parameter of  $\sim 0.5$  should provide low beam walk and therefore high cavity stability.

The required 3-m length cavity is significantly longer than that employed in our bench-top setup (which has  $L=0.75$  m) and than those used by most researchers. Therefore, as a means of characterization, we have setup a 3-m length in ambient air (i.e. not connected to our vacuum system) on the bench-top. Fig. 6a shows initial ring-down traces obtained from this cavity using the same detection system as we employ for our  $l=0.75$  m cavity. Clearly large noise is present in the ring-down signals. The noise arose because for the longer cavity, the laser pulse duration ( $\sim 7$  ns) is shorter than the cavity round-trip time of 20 ns ( $= 2 \times 3\text{m} / 3 \times 10^8 \text{ m/s}$ ). In such cases, individual “bounces” are detected within the ring-down signal, with the “bounces” corresponding to the light pulse moving back-and-forth between the cavity mirrors. (An individual “bounce” is detected each time the light pulse reaches the

exit mirror.) The inset to Fig. 6a shows these bounces when looking at a portion of the overall ring-down signal with higher time resolution. The high-frequency bounces appear as “noise” in the ring-down signals and limit our ability to fit them with exponentials. The problem was alleviated by increasing the response time (RC time constant) of the detection system, which was achieved by increasing the input impedance of the oscilloscope from 50Ω to 1000Ω (Fig. 6b). With this configuration, the response time (~50 ns) is sufficiently slow to remove the individual bounces, yet fast enough to not affect the ring-down envelope (exponential fit). The resulting ring-down traces and times offer no apparent decrease in stability, or sensitivity, as compared to those from the shorter cavity.

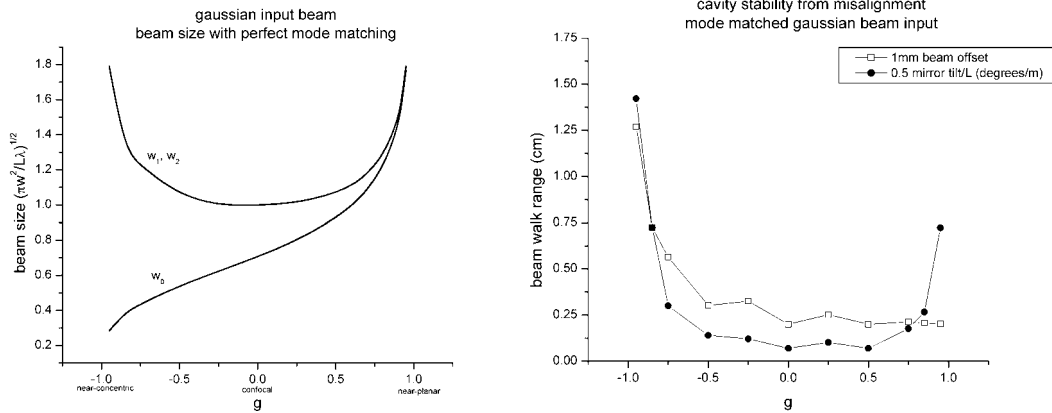


**Figure 5. Numerical simulations beam size (in center of cavity) versus cavity  $g$ -parameter (left), and beam walk versus cavity  $g$ -parameter (right)<sup>12</sup>.**

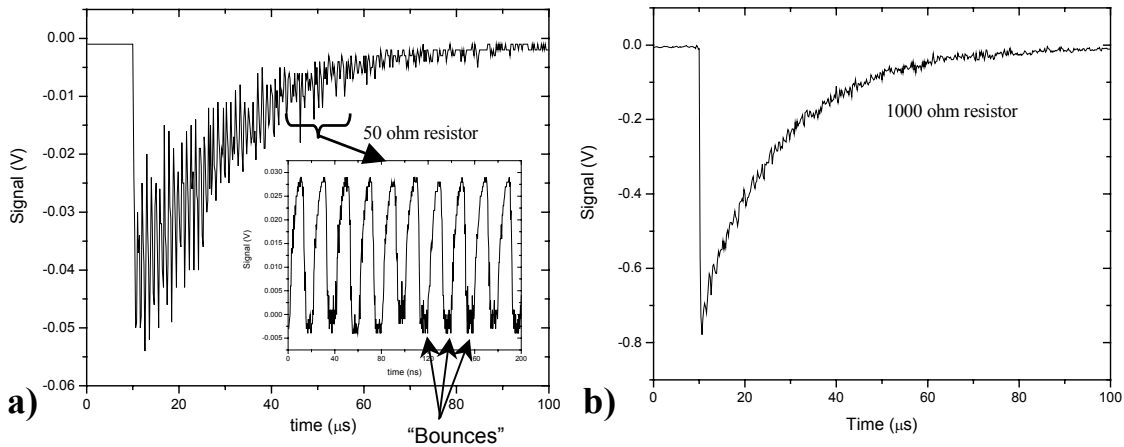


**Figure 6. a) Individual ring-down traces obtained with 50 Ω input impedance. Inset (ns time base) shows that the noise is due to detection of individual “bounces” (spaced by the cavity round-trip time of 20 ns). b) Smooth ring-down signals are obtained by increasing the input impedance to 1000 Ω.**

### B. Design of Cavity Arms

Specially designed cavity arms are required to integrate the ring-down cavity with the JPL vacuum chamber. In addition to allowing for precise adjustment of the cavity alignment, we also require a way to combat potential reduction of effective cavity finesse (and CRDS sensitivity) due to mirror contamination from condensed bismuth or sputter products. An initial design for the chamber arms is shown in Fig. 7. Only one arm is shown, but two identical arms will be used, one on each side of the chamber. Key design features are as follows. Almost all component are available “off-the-shelf”, allowing for easy, low-cost assembly. Gate-valves are used to allow removal of mirrors (for cleaning or replacement of mirrors) without disrupting the chamber vacuum. Mirrors are vacuum-sealed against adjacent O-rings. Mirror alignments adjustment is achieved using three set-screws that press

against a brass ring on the back of the mirrors, allowing changes in the mirror angles by changing the compression of the O-ring. A re-entrant tube containing a series of irises is used to protect the mirrors against being contaminated by condensable products.

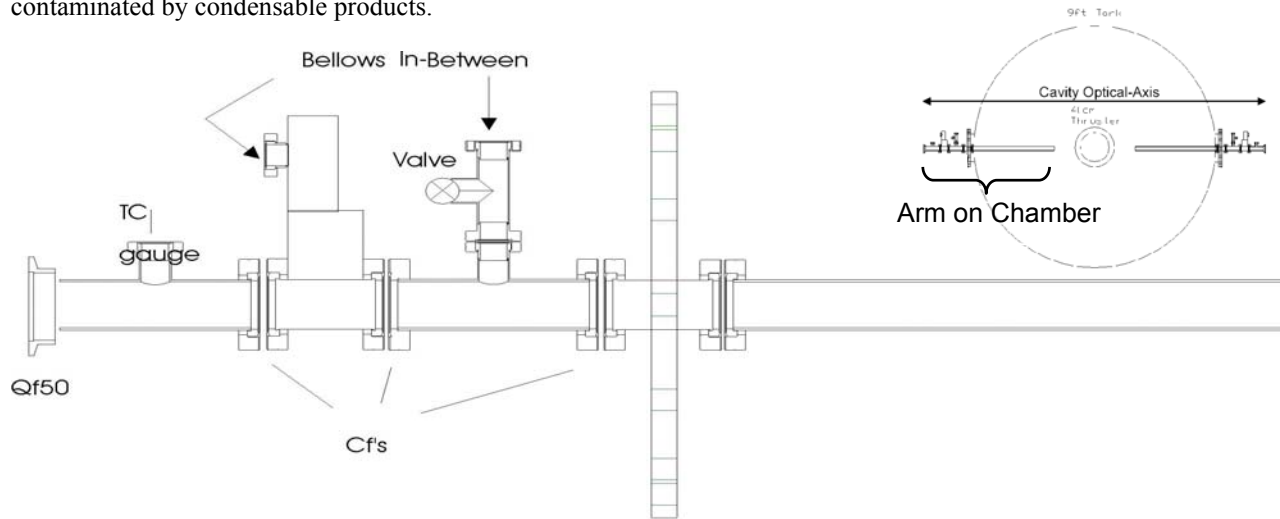


Figure 7. Schematic design of a single cavity arm. Inset (top right) shows schematic of a pair of arms mounted on a chamber. Legend: TC – thermocouple gauge, Cf – 2-3/4 conflat flanges, Qf50 - size 50 quick flange.

### C. VHITAL Thruster Measurements

The CRDS detection system will be implemented to study the VHITAL thruster on the JPL vacuum chamber. CRDS measurements of sputtered molybdenum within the plume of the thruster will be performed. The approach is schematically illustrated in Fig. 8. Measurements will be performed as the thruster operating conditions (set points) are varied. The thruster will be moved on a translation stage in order to probe different chords and yield (via Abel inversion) radial profiles of Mo concentration within the plume. These measurements will provide information on how thruster erosion (and lifetime) may vary with thruster operating conditions. The measurements will also be used to validate computational models addressing thruster erosion. Though we will only measure molybdenum erosion (from Mo guard rings), other materials, such as graphite, likely will be used as the actual guard-ring material owing to their lower erosion rates. The CRDS measurements of Mo will contribute to validation of the overall erosion modeling approach and thus will be beneficial towards evaluation of all species of interest.

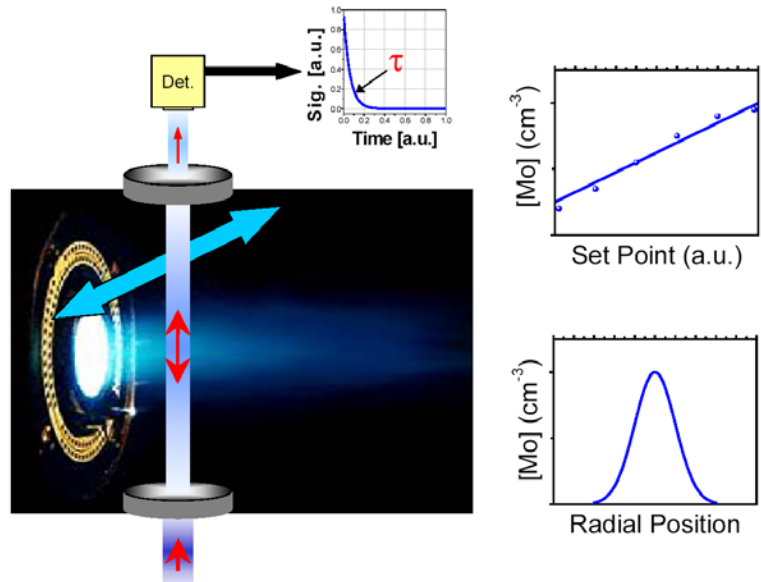


Figure 8. Approach to CRDS measurements in plume of VHITAL thruster. A CRDS cavity will surround the plume (actually with horizontal orientation), and measure Mo within the plume.

## V. Summary

The cavity ring-down spectroscopy (CRDS) technique provides a tool to quantitatively study sputter erosion of the VHITAL thruster. The CRDS diagnostic will be used to measure sputtered molybdenum in the thruster plume. The CRDS measurement results will be used together with other diagnostics and numerical modeling as part of the overall lifetime assessment program. In this work we have presented our bench-top set-up for diagnostic development and discussed our CRDS measurements of sputtered molybdenum number density and velocity. The detection limit achieved is expected to be very adequate for measurements on the VHITAL thruster. We have also presented the design of chamber arms to be used for the ~3m length cavity needed to study the VHITAL thruster.

## Acknowledgments

The research was funded by NASA's Exploration Systems Missions Directorate, managed by John Warren, Associate Director for Advanced Systems and Technology, Prometheus Nuclear Systems and Technology Program. The authors also acknowledge Mark Butweiller's technical help with the apparatus and apparatus design.

## References

1. Marrese-Reading, C. et al, "The VHITAL Program to Demonstrate the Performance and Lifetime of a Bismuth-Fueled Very High Isp Hall Thruster," AIAA-2005-4564, *41<sup>st</sup> AIAA/ASME/SAE/ASEE Joint Propulsion Conference*, Tucson, AR, July 2005.
2. Marrese-Reading, C. et al, "Very High Isp Thruster with Anode Layer (VHITAL): An Overview," *AIAA Space Conference*, San Diego, CA, September 2004.
3. Kolasinski, R.D. and Polk, J.E., "Characterization of Cathode Keeper Wear by Surface Layer Activation," AIAA Paper No. 2003-5144, *39th AIAA Joint Propulsion Conference*, Huntsville, AL, 2003.
4. Busch, K.W. and Busch, M.A. "Cavity-Ringdown Spectroscopy - ACS Symposium Series 720, Vol. 720, 1999.
5. Berden, G., Peeters, R. and Meijer, G. "Cavity Ring-Down Spectroscopy: Experimental Schemes and Applications," *Int. Reviews in Physical Chemistry*, Vol.19, No.4, p. 565-607, 2000.
6. Surla, V., Wilbur, P.J., Johnson, M., Williams, J.D., and Yalin, A.P. "Sputter erosion measurements of titanium and molybdenum by cavity ring-down spectroscopy," *Review of Scientific Instruments*, Vol.75, No.9, p. 3025-3030, 2004.
7. Yalin, A.P., Surla, V., Butweiller, M., Williams, J.D. "Detection of Sputtered Metals using Cavity Ring-Down Spectroscopy," *Applied Optics*, expected: Vol. 44, No. 30, 2005.
8. Yalin, A.P., and Surla, V. "Velocity Measurements by Cavity Ring-Down Spectroscopy," *Optics Letters* (to be published).
9. Zalicki, P., and Zare, R.N. "Cavity ring-down spectroscopy for quantitative absorption measurements," *Journal of Chemical Physics*, Vol. 102, No.7, p. 2708-17, 1995.
10. Yalin, A.P., and Zare, R.N. "Effect of Laser Lineshape on the Quantitative Analysis of Cavity Ring-Down Signals," *Laser Physics*, Vol.12, No.8, p. 1065-1072, 2002.
11. Hudson, W.R. and Banks, B.A. AIAA Paper No. 73-1131, in 10th AIAA Electric Propulsion Conference, Lake Tahoe, NV, 1973.
12. Spuler, S. and Linne, M. "Numerical analysis of beam propagation in pulsed cavity ring-down spectroscopy," *Applied Optics*, Vol.41, No.15, p. 2858-2868, 2002.
13. Siegman, A.E., *Lasers*. 1986, Mill Valley: University Science Books. 1283.